OXYGEN-FREE COMPOUND CASTING OF ALUMINUM AND COPPER IN A SILANE-DOPED INERT GAS ATMOSPHERE: A NEW APPROACH TO INCREASE THERMAL CONDUCTIVITY

Andreas C. Fromm, Khemais Barienti, Armin Selmanovic, Susanne E. Thürer, Florian Nürnberger, Hans Jürgen Maier and Christian Klose

Institut für Werkstoffkunde (Materials Science), Leibniz Universität Hannover, An der Universität 2, 30823 Garbsen, Germany

Abstract

Novel aluminum-copper compound castings devoid of oxide layers at the interface between the joining partners were developed in order to increase the thermal conductivity of the hybrid component. Due to the natural oxide layers of both aluminum and copper, metallurgical bonds between such bi-metal castings cannot be easily achieved in conventional processes. However, in an atmosphere comparable to extreme high vacuum created by using silane-doped inert gas, metallurgical bonds between the active surfaces of both aluminum and copper can be realized without additional coatings or fluxes. An intermetallic was created between aluminum and copper. Thus, very high thermal conductivities could be obtained for these hybrid castings, exceeding those of conventionally joined samples considerably. The intermetallic phase seams emerging between the joining partners were investigated using scanning electron microscopy and X-ray diffraction. The reduction of casting temperatures resulted in narrower intermetallic phase seams and these in turn in a much lower contact resistance between the two joining partners. This effect can be utilized for increasing the heat transfer capabilities of compound casting components employed for cooling heat sources such as high-power light-emitting diodes.

Keywords: bi-metal compounds, extreme high vacuum, microstructure, intermetallic phases, cooling components
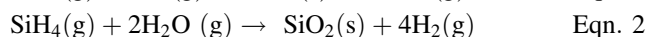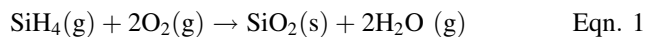
Introduction

The performance of many devices such as high-power light-emitting diodes decreases with increasing temperatures.[1] To counteract this, cooling solutions offering both high performance and high cost efficiency at the same time are necessary for modern electronic components. These two requirements can be met with compound heat sinks made of aluminum, contributing low density and good thermal conductivity, and copper, providing high thermal conductivity. A major disadvantage of conventional compound heat sinks made of these two materials is the high contact resistance resulting from a gap that is typically formed along the interface between copper and aluminum. These metals are often joined mechanically, with thermal paste used to bridge the gap, or by soldering. But the thermal paste has a relatively low thermal conductivity itself and the soldering process is often not able to fill the entire area between the two joining partners.[2] Other typical methods of solid-state joining of aluminum and copper, such as diffusion welding,[3,4] cold rolling,[5–8] explosive welding,[9,10] extrusion,[11,12] etc., all have certain disadvantages in comparison to compound casting, e.g. in terms of the dimensions of the processable specimens as well as the time and effort required or the high production cost. Against this background, casting with its potential to overcome the described limitations[13] was the process of choice in this study.

Compound casting is classified as a process in which a solid and a liquid metal form a metallic bond via diffusion.[14] However, creating a metallurgical bond that provides high thermal conductivity can generally not be achieved by directly casting liquid aluminum onto a solid

copper insert in a mold, since oxide layers on the surfaces of the two metals impede the necessary diffusion process.[13] A possible solution is to apply intermediate layers onto the copper insert piece, e.g. low-melting alloys based on zinc which are partially washed away and dissolved in the molten aluminum, establishing direct contact between the juvenile metallic surface of the copper and the aluminum melt.[15] Similarly, copper inserts can be coated with tin to create the necessary wetting between the two joining partners[16] or copper inserts can be integrated into a pattern for lost foam casting before being joined with aluminum.[17] Another approach is to use conventional fluxes and pickle, which prevent the formation of new oxide layers on the copper insert.[18,19] However, these chemicals are toxic and harmful to the environment.

In this study, a novel approach was developed to prevent the formation of oxide layers on the materials prior to casting that occur in an inert gas atmosphere. Since even high-purity inert gases such as argon 5.0 (99.999% purity) still contain approximately 0.05 ppmv oxygen, their use cannot prevent the immediate re-formation of an oxygen monolayer on a deoxidized metal surface.[20] In contrast, the approach employed in the present study aims at eliminating the formation of oxide layers on both the copper inserts as well as on the aluminum melt by reducing the oxygen activity to extremely low levels. This way, collisions of oxygen molecules with the deoxidized surface can be avoided at least for the duration of the actual casting process. As calculated by Holländer et al.,[20] a thermodynamic oxygen activity as low as $< 10^{-32}$ at 800 °C could potentially be achieved under ideal conditions, such as those that exist in an extreme high vacuum. Due to the challenges of generating an extremely high vacuum, the approach pursued here is to create an XHV-adequate atmosphere by doping high-purity argon (99.999% Ar) with small amounts of SiH_4 (monosilane). In the inert gas atmosphere, the silane reacts with the residual oxygen and water to form non-reactive silane dioxide, thus removing both educts from the environment:[21]

$$SiH_4(g) + 2O_2(g) \rightarrow SiO_2(s) + 2H_2O\ (g) \qquad \text{Eqn. 1}$$
$$SiH_4(g) + 2H_2O\ (g) \rightarrow\ SiO_2(s) + 4H_2(g) \qquad \text{Eqn. 2}$$

In this study, compound casting was conducted in such an XHV-adequate atmosphere. The objective was to develop novel aluminum-copper compounds with a continuous metallurgical bond, and without any impeding oxide layers at the interface of the joining partners. Thus, the resulting contact resistance between aluminum and copper should mainly be governed by the characteristics of the local microstructure of the compound zone, i.e. types and thicknesses of intermetallic phases and diffusion zones. In particular, the temperature regime of the casting process was varied to investigate the impact of the casting parameters on the local microstructure as well as the thermal conductivity in the compound zone under XHV-adequate conditions. It is important to emphasize that the current study aims at gaining a profound understanding of the fundamental mechanisms governing the oxide-free casting process. Thus, pure aluminum was used as the cast material, which provided a benchmark in terms of achieving high thermal conductivity. With respect to application, the new deoxidization technique offers the advantage that it can be integrated into industrially relevant casting processes, as the XHV-adequate atmosphere is only required inside the mold. Likewise, the new process can be adopted for typical aluminum cast alloys, since the prevention of the Al_2O_3 layer formation in an XHV-adequate atmosphere is based on thermodynamics and therefore works in the same way for Al-Si alloys such as A356 as for the pure aluminum used here.

Materials and Methods

Basic Materials

Cylindrical copper inserts with the dimensions Ø 31.8 mm × 2 mm were cut from a cold rolled oxygen free (OF) copper plate (Hans-Erich Gemmel & Co. GmbH, Berlin, Germany) by wire electrical discharge machining (EDM). The copper inserts featured a purity level of > 99.65% and were cleaned with ethanol prior to the compound casting experiments. The cast aluminum provided by Hydro Aluminium High Purity GmbH (Grevenbroich, Germany) had a purity of > 99.87%. Table 1 shows the chemical compositions of the metals used in this study as measured with a spark spectrometer.

The aluminum ingots were heated to 200 °C to remove water residues and then cut into small pieces weighing 30–40 g. Subsequently, both the copper insert and the aluminum pieces were transferred into a glovebox with an XHV-adequate atmosphere via an airlock. Inside the glove box, the native oxide layer of the copper inlay was mechanically removed by grinding, using first 500 grit and then 1200 grit abrasive papers.

Table 1. Mean Chemical Composition (wt.-%) of the Samples as Measured by Spark Spectrometry

	Cu	Al	Si	Fe	Zn	B	others
Copper	> 99.65	0.007	0.0005	0.003	0.015	0.0002	< 0.3
Aluminum	0.022	> 99.87	0.0094	0.012	0.026	0.014	< 0.05

Compound Casting in an XHV-Adequate Atmosphere

Compound casting was conducted in a glovebox (Labmaster 130, Mbraun GmbH, Munich, Germany), that was previously flooded with argon 4.8 (99.998% purity) to displace the air inside the entire box. To remove any residual oxygen and water, a prefabricated mixture of 99 mol-% argon 5.0 (99.999% purity) and 1 mol-% monosilane provided by Messer Industriegase GmbH (Bad Soden am Taunus, Germany) was infused. This procedure allowed for an inert gas atmosphere with an extremely low oxygen activity (reduction to $2 \cdot 10^{-18}$ vol.-%) in the process zone. The actual oxygen activity was continuously monitored with a calibrated λ-probe to make sure that an oxygen-free, XHV-adequate atmosphere was reliably established.

The aluminum-copper compounds were produced by gravity die-casting. For this purpose, a casting device featuring a manually operated tilting graphite crucible with a filling volume of 130 ml was employed. The crucible and the aluminum placed inside were heated by a resistance heater coil whose temperature was controlled by means of a type-K thermocouple. The mold for the copper inserts as well as the casting channel had previously been coated with boron nitride (Henze Boron Nitride Products AG, Lauben, Germany). The mold had a drilled hole for the copper insert and another one for a thermocouple (type-K). Additionally, the temperature on the copper surface was measured with a contact thermocouple (type-K) before pouring the liquid aluminum onto it. Furthermore, a tube allowing direct doping of monosilane into the mold was installed. This way, the copper insert can be immersed in excess monosilane during heating in the mold, thus preventing its possible re-oxidation caused by gases released from the mold.

The casting experiments were performed with various temperature regimes to determine the influence of both the crucible and mold temperatures on the microstructure in the bonding zone between copper and aluminum. The minimum temperatures required to establish a successful bond in an XHV-adequate atmosphere had been determined in preliminary tests. For the experiments described here, the crucible temperature was varied between 750, 775, and 800 °C and the mold temperature from 300 °C to 500 °C at intervals of 50 °C. These temperatures cover the ranges typically used for the crucible and the mold when aiming to create a bond between aluminum and copper.[16]

The crucible was filled with 115 g aluminum at room temperature and then heated to the target temperature with a heating rate of 45 °C/min. The mold was heated with a heating rate of 20 °C/min. Depending on the selected casting parameters, the heating of the mold was timed to achieve both the selected crucible and mold temperatures simultaneously. After the target mold temperature was reached and the aluminum casting material had melted completely, the deoxidized copper insert was placed in the mold. A subsequent holding time of 5 min allowed for reaching stationary conditions. Finally, the molten aluminum was poured into the casting mold directly onto the copper insert and the heating was deactivated.

Microstructural Characterization of the Aluminum-Copper Compounds

After cooling to room temperature, the aluminum-copper compound castings were removed from the glovebox and prepared for analysis. The specimens with an outer diameter of 31.8 mm were shortened by turning until the copper part had a plane-parallel thickness of 1 mm ± 0.1 mm in order to allow comparisons of the effects of different casting regimes. Four samples with a diameter of 10 mm each and three samples with a diameter of 8 mm each were then cut from the compounds by wire EDM. Figure 1a illustrates the sample extraction positions from the cast compounds. Each specimen was turned plane-parallel to a total thickness of 3 mm (Figure 1b). The samples with Ø 8 mm were used for microstructural characterization by scanning electron microscopy (SEM) and X-ray diffraction (XRD) and those with Ø 10 mm for the thermal conductivity measurements.

For microstructural investigations, cross sections of the samples were metallographically prepared and etched. Grinding was performed with emery paper with grit sizes of 220, 400/500, 1200, and 2500. Finally, the samples were polished with diamond suspensions with grit sizes of 6 μm and 3 μm. Etching was performed using a hydrofluoric acid (10%) for aluminum and a mixture of potassium disulfite (25% to < 30%) and sodium thiosulfate pentahydrate (1% to < 5%) for copper. Images of the polished and etched specimens were taken by a BX53M optical microscope (Olympus Europa SE & Co. KG, Hamburg, Germany) and a DM4000M optical microscope (Leica Microsystems GmbH, Wetzlar, Germany).

To investigate the chemical composition of the compound zone, the polished samples were examined with a Zeiss Supra VP 55 field-emitter scanning electron microscope (SEM). For recording images dominated by material contrast, a backscattered electron detector (BSD) was employed. The chemical compositions were determined by energy dispersive X-ray spectroscopy (EDS) using a detector (Bruker AXS GmbH, Karlsruhe, Germany) in the SEM.

Quantitative identification of the phase stoichiometry inside the compound zone was performed with an X-ray diffractometer (D8 Discover, Bruker AXS GmbH, Karlsruhe, Germany). Specifically, a symmetric 2-theta
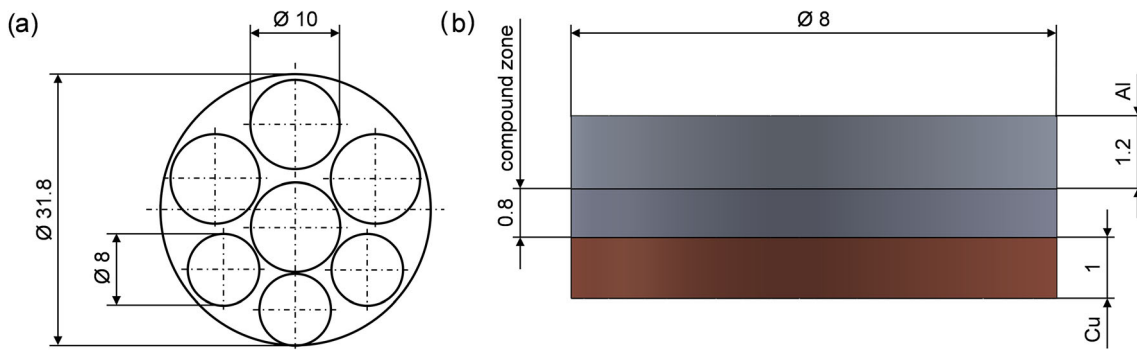
Figure 1. *(a) Top view showing locations of the ⌀ 8 mm and ⌀ 10 mm specimens; (b) corresponding side-view with target layer thicknesses after machining.*

setup with Co Kα radiation (wavelength of 1.788 Å) was employed. The X-ray beam was narrowed using a 0.3 mm collimator and the diffracted intensities were recorded with a VÅNTEC-500 2D detector at a step size of 20° for coupled 2-theta/theta measurements. Given the assumption that at least some of the intermetallic phase seams between the joining partners would only be a few μm wide,[13,22] the samples were cut at an angle of 80° (Figure 2a) by wire EDM to effectively enlarge the area of the compound zone. As shown schematically in Figure 2b, this allowed to probe the compound zone by XRD without the substrates contributing to the signal. For XRD analysis, five measuring points (MP) were placed across the compound zone of each specimen (Figure 2c). The measurements were thus performed on copper (MP 1) and the phase seam (MP 2–4) as well as on aluminum (MP 5). Evaluation of the diffraction patterns was performed using EVA 4.0 software (Bruker AXS GmbH, Karlsruhe, Germany).

Thermal Conductivity

The thermal conductivity of the castings was measured indirectly by irradiating the bottom surface of the samples with a xenon flash measuring device (LFA 447 from Netzsch-Gerätebau GmbH, Selb, Germany). The resulting temperature change of the upper surface of the sample was recorded with an indium antimonide infrared detector, which was cooled with liquid nitrogen. Prior to the

measurements, the samples were coated with graphite on both sides to improve the absorption of the energy and the emission of infrared radiation to the detector. The thermal diffusivity was calculated using the pulse correction according to Cowan.[23] The radiation losses as well as the convection on the surface were considered for the calculation.

Based on the measured thermal diffusivity a, the thermal conductivity λ can be calculated as[24]:

$$\lambda = a \cdot c_{p} \cdot \rho \qquad \text{Eqn. 3}$$

Where, c_{p} is the specific heat capacity and ρ is the density of the measured material.

In the present study, the density of the samples was determined using an MK 2000 density measuring scale (MK Industrie-Vertretungen GmbH, Stahlhofen am Wiesensee, Germany). The specific heat capacity was determined using a reference sample whose respective values were known. Following this procedure, the thermophysical properties were determined for each base material, i.e. aluminum and copper, and the various multilayer samples. For measuring the latter, the exact layer thicknesses of the whole compound zone were determined in the SEM. Since it was not possible to measure the compound zone exclusively, the thermal conductivity of the compound zone was estimated using a simplified
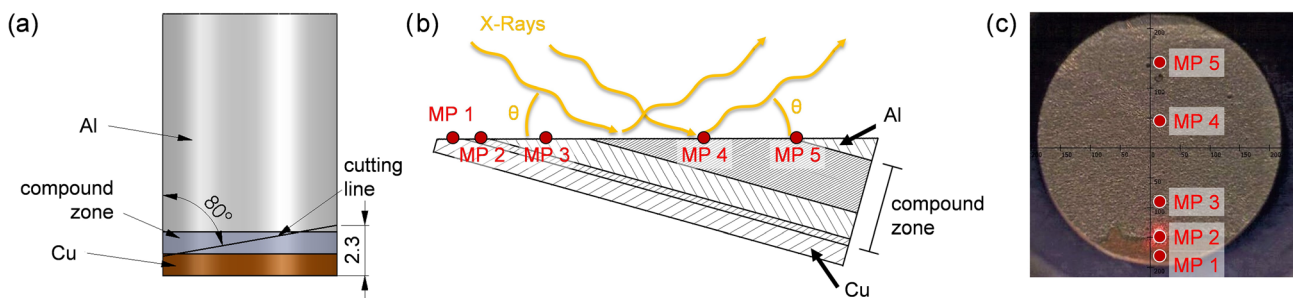
Figure 2. *(a) Sectioning of the sample at an angle of 80° to enlarge the width of the compound zone; (b) XRD measurement of the different areas of the compound zone; (c) actual location of the measuring points for the XRD measurement.*

model. Assuming that the aluminum-copper compounds consist of only two layers (aluminum and copper), the contact resistance between the copper insert and the cast aluminum and thus the thermal conductivity of the compound zone can be calculated (using Eqn. (4)). In the calculation, the layer thicknesses d_i and the average values of the previously measured thermal conductivities λ_i of the pure metals aluminum and copper were used. The calculated contact resistance R is the thermal resistance of the compound zone. The relationship between the thickness of the compound zone and the measured value was calculated as[24]:

$$\lambda_{\text{compoundzone}} = \frac{d_{\text{compoundzone}}}{R} \qquad \text{Eqn. 4}$$

In order to better assess the influence of the compound zone on the thermal conductivity between the copper insert and the aluminum casting material, the combined thermal conductivity was also determined. The thermal resistances of the compound zone ($R_{\text{compoundzone}}$) and the aluminum casting material (R_{Al}) were combined as

$$\lambda_{\text{compoundzone+Al}} = \frac{d_{\text{compoundzone}} + d_{\text{Al}}}{R_{\text{compoundzone}} + R_{\text{Al}}} \qquad \text{Eqn. 5}$$

The combined thermal conductivity can potentially reach the thermal conductivity of the cast material, so ideally, the thermal resistance of the compound zone tends to zero.

To shed light on the influence of different casting parameters (i.e., mold temperature and crucible temperature) on the thermal resistance of the compound zone, at least three samples of each parameter combination were measured to calculate average thermal conductivity values. Since thermal conductivity depends on the actual temperature, thermal diffusivity was measured in the temperature range between 25 °C and 200 °C, corresponding to the typical operating temperature range of heat exchangers. Higher temperatures could lead to increased diffusion processes, which would permanently affect the local microstructure of the compound zone.[25]

Results

Process Temperatures and Limitations

The temperatures of the aluminum melt and the solid copper insert were monitored during the casting experiments. The process parameters resulting in formation of a metallurgical bond are provided in Table 2.

The temperature of the crucible (Figure 3a) heated by means of a resistance coil was approx. 57 °C higher than the temperature of the aluminum melt for all castings.

Table 2. Suitable Process Temperatures for Formation of Metallurgical Bonds; Process Limit at Lower Temperatures is Marked in Blue

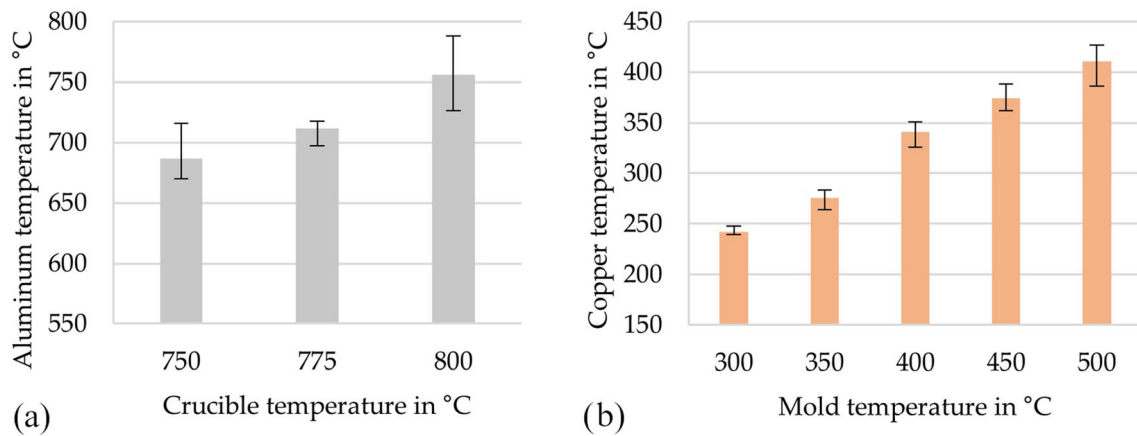| Mold temperature Crucible temperature	500 °C	450 °C	400 °C	350 °C	300 °C
800 °C	✔	✔	✔	✔	✔
775 °C	✔	✔	✔	✔	X
750 °C	✔	✔	✔	(✔)	X

✔: Bonding, X: No bonding, (✔): Occasional bonding (not repeatable)

Figure 3b shows that the mold temperature was also higher than the copper insert temperature. On average, the mold temperature exceeded the copper insert temperature by approx. 70 °C. This suggests that the process limit shown for the crucible as well as the mold temperatures in Table 2 is even lower if the actual contact temperatures between the bond partners are considered.
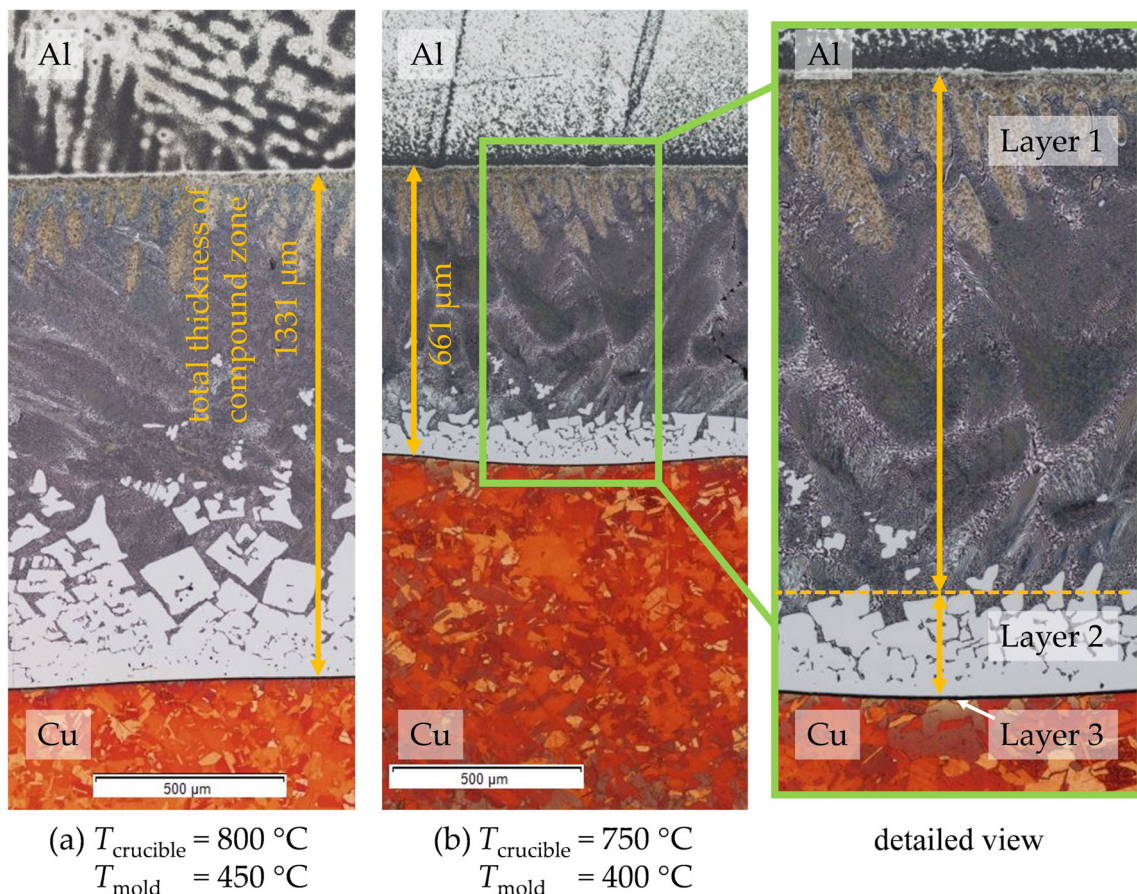
Characterization of the Compound Zone

Figure 4 shows light microscopic images of representative aluminum-copper compounds produced using different casting parameters. While copper can be recognized by its reddish colors, the cast aluminum appears in different shades of gray. In both samples, a distinct compound zone was formed, divided into different layers. With increasing casting temperatures, the overall thickness of the compound zone also increased. For the specimen cast at a crucible temperature of 800 °C and a mold temperature of 450 °C (Figure 4a, a maximum layer thickness of ≈ 1.3 mm was observed. Lower temperatures led to a reduction of layer thicknesses, as shown exemplarily in Figure 4b with a specimen cast featuring a crucible temperature of 750 °C and a mold temperature of 400 °C. Here, a layer thickness of ≈ 0.7 mm was obtained.

The dependence of the built thickness of the composite zone on the given temperatures of the crucible and the mold is illustrated in Figure 5. It is evident that the temperature of the mold, and thus the one of the copper insert, had a greater influence on the total thickness of the compound zone than the temperature of the aluminum melt. For this reason, employing different crucible temperatures while keeping the mold temperature constant resulted in only slightly differing the thicknesses of the compound zones. Similarly, a tendency towards a higher overall thickness of the compound zone was also observed for increasing mold temperatures combined with a constant crucible temperature. By contrast, it was not possible to create a full bond at a low mold temperature of only 300 °C at a crucible temperature lower than 800 °C.

Figure 3. Comparison of the nominal casting temperatures and the measured temperatures of aluminum (a) and copper (b).


(a) $T_{\text{crucible}} = 800\,°C$
$T_{\text{mold}} = 450\,°C$

(b) $T_{\text{crucible}} = 750\,°C$
$T_{\text{mold}} = 400\,°C$

detailed view

Figure 4. Representative light microscopic images of etched specimens: (a) $T_{crucible}$ = 800 °C, T_{mold} = 450 °C and (b) $T_{crucible}$ = 750 °C, T_{mold} = 400 °C.

SEM and XRD Phase Analysis

Based on the aluminum-copper phase diagram, the chemical compositions obtained from the EDS provided initial indications of the phases present. The sample with the largest compound zone of $\approx$ 1.3 mm (T_{crucible} = 800 °C, T_{mold} = 500 °C) is shown exemplarily in Figure 6. The three differently shaped layers already detected by light

microscopy were also evident in the SEM. In order to identify the different phases formed between copper and aluminum, EDS linescans were performed.

Given the aluminum base material, the first layer of the microstructure according to literature (e.g., Tavassoli et al.,[22] Greß et al.[26]) should be a eutectic structure consisting of a copper-rich aluminum solid solution (α-Al)
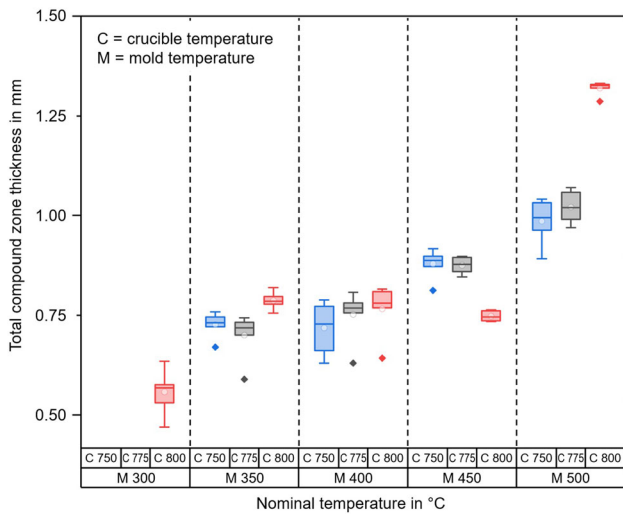
Figure 5. Measured total thicknesses of the compound zones of samples cast at different temperature regimes.

and the θ-phase (Al$_2$Cu). This is also the case with the compound castings created in XHV-adequate environment here: The BSD image (Figure 6a) of the first layer reveals a thin lamellar microstructure characteristic of a eutectic microstructure. According to the EDS linescan (Figure 6b),

the eutectic microstructure consists of α-aluminum with a copper content of about 17 at.-% and the composition of the intermetallic fits the θ-phase (Al$_2$Cu). In between the second layer – containing the θ-phase—and the copper substrate, another very narrow third layer was detected (Figure 6c). This additional intermediate layer was also described by Tavassoli et al.[22] In the EDS analysis, local element enrichment was detected. Specifically, the EDS analyses showed a chemical composition of about 35 at.-% aluminum and 65 at.-% copper for area "B" (Figure 6d). In contrast to region "C", which featured irregular thickness, region "B" was more homogeneous across the whole sample. The corresponding diffraction patterns found in the XRD measurements were more distinct and the inter-metallic γ-phase (Al$_4$Cu$_9$) could be assigned to this region (PDF 00-024-0003[27]). The third region "C" had a chemical composition of about 47 at.-% aluminum and 53 at.-% copper, indicating the presence of the η$_2$ (AlCu) phase. Between the regions B and C, another very thin and discontinuous layer, marked by (*) in Figure 6c, could be detected in some of the BSD images. Its composition will have to be elucidated in a future investigation since the EDS analyses did not provide the necessary lateral resolution due to the excitation bulb.
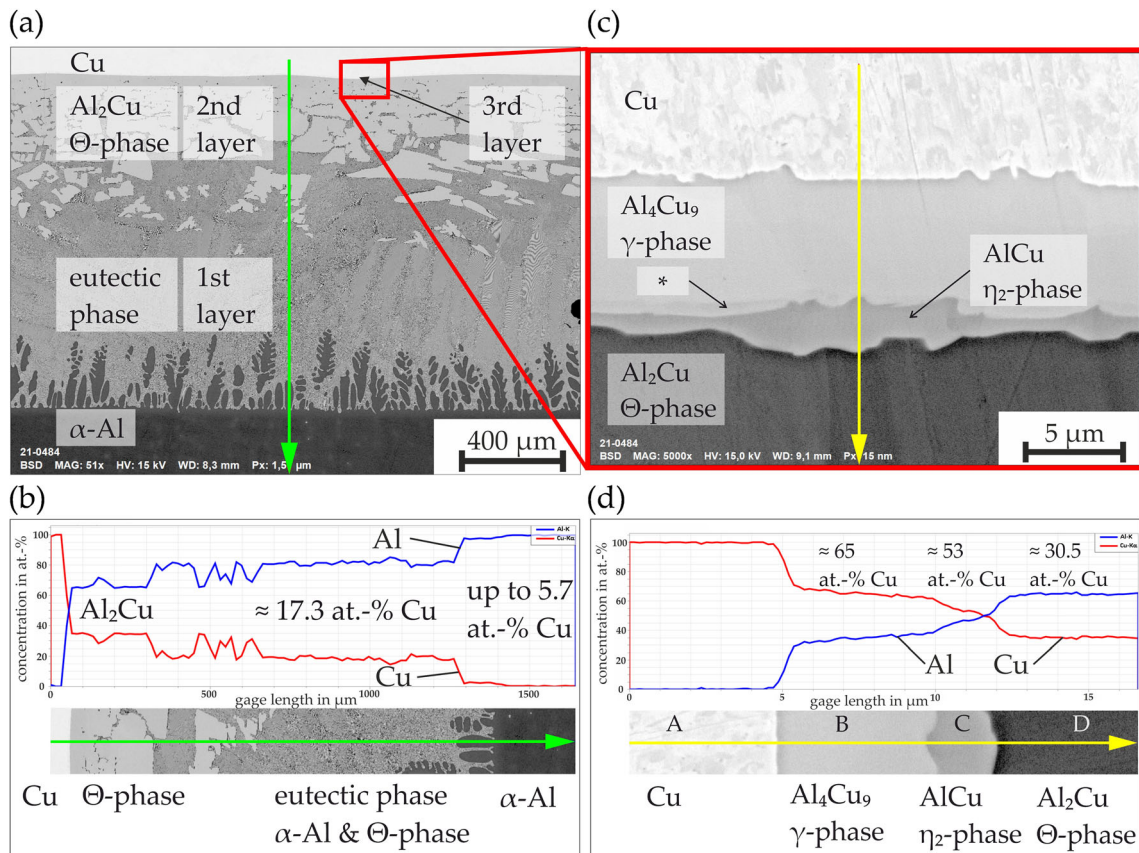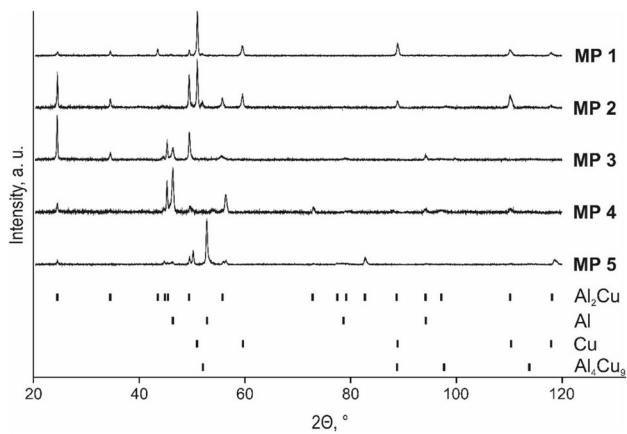

Figure 6. (a) BSD overview image and corresponding (b) EDS linescan (trace is marked by arrow) with element concentration in at.-%, T$_{crucible}$ = 800 °C, T$_{mold}$ = 500 °C, (c) BSD image providing a detailed view of the 3rd layer and corresponding (d) EDS linescan with element concentration, (*) unidentified layer.

To further substantiate the findings regarding the phase compositions, XRD analysis was performed on the prepared specimen. Diffractograms obtained at the different measuring points MP 1-5 are shown in Figure 7. Employing the ICDD PDF2016 database,[27] the diffraction patterns can be assigned to the θ-phase (Al₂Cu) (PDF 01-076-3073) as well as to α-Al (PDF 03 065 2869). The incorporation of Cu atoms into the Al lattice causes a distortion resulting in a peak shift towards larger diffraction angles. The copper-containing aluminum thus featured a smaller unit cell than the base material. A decrease of the lattice constant along with increasing copper content was already demonstrated for copper-containing aluminum solid solutions.[28] Consequently, the diffraction peaks at 2θ = 46° and 53.5° (Figure 7) can be assigned to the copper-rich aluminum solid solutions created by compound casting in XHV-adequate atmosphere.

Thermal Conductivity

For measuring the thermal conductivity of the multilayer specimens, the outer layers (here: aluminum and copper) had to be fully characterized to calculate the contact resistance of the phase seam. Thermal conductivity λ was calculated using Eqn. (3). First, the averaged thermal diffusivities of three samples from each bulk material were measured. Since the standard deviations of the respective mean values were below 1 mm²/s for the thermal diffusivity and below 0.01 J/(g·K) for the specific heat capacity, the error bars in Figure 8 can barely be recognized. It was observed that the thermal diffusivity of copper first increases and then decreases with increasing temperature, whereas that of aluminum decreases continuously with increasing temperatures (Figure 8).
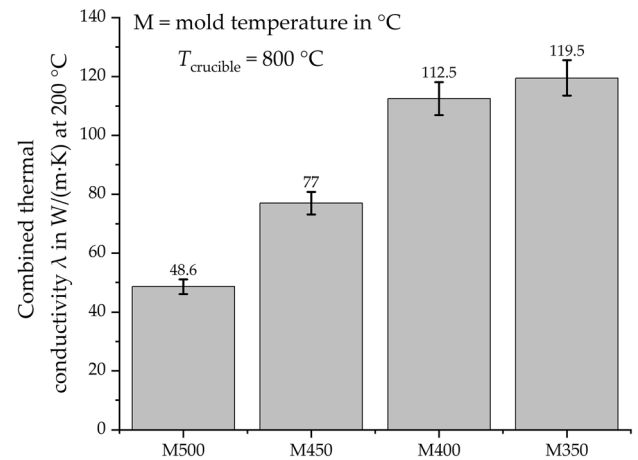
Thermal conductivities of the compound zones of the different specimens as well as the combined thermal conductivities were determined using Eqns. (4) and (5). Figure 9 shows the thermal conductivities calculated for

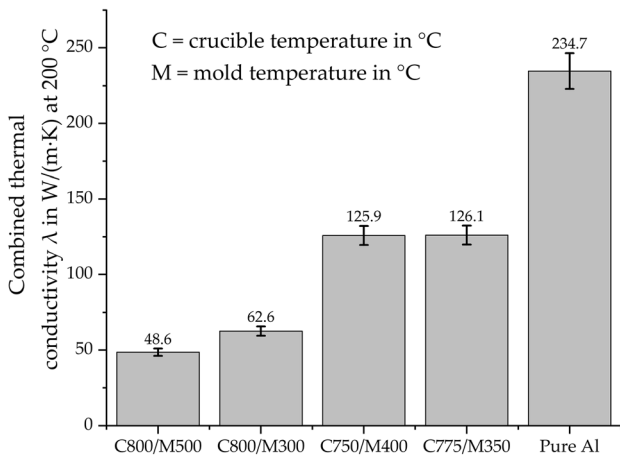**Figure 8. Thermal conductivities of the bulk materials depending on ambient temperature.**

Figure 9. Combined thermal conductivity at different mold temperatures, mean values with n = 3.

the composite zones as a function of the mold temperature used. For the specimens produced at a nominal crucible temperature of 800 °C, lower mold temperatures were found to be resulting in higher thermal conductivities of the specimens.

The range of thermal conductivities that could be achieved for the different aluminum-copper compounds produced are shown in Figure 10. Depending on the casting parameters, different thicknesses of the compound zones were induced, which in turn resulted in a substantial change of the thermal conductivity. It needs to be noted that due to the usual local process fluctuations, it is not yet possible to produce compound zones featuring homogeneous thicknesses over the entire cross-section, which impairs the overall performance of the compound castings.

Using Eqn. (5), the maximum possible combined thermal conductivity of an aluminum-copper compound is obtained for a contact resistance of zero, corresponding to the
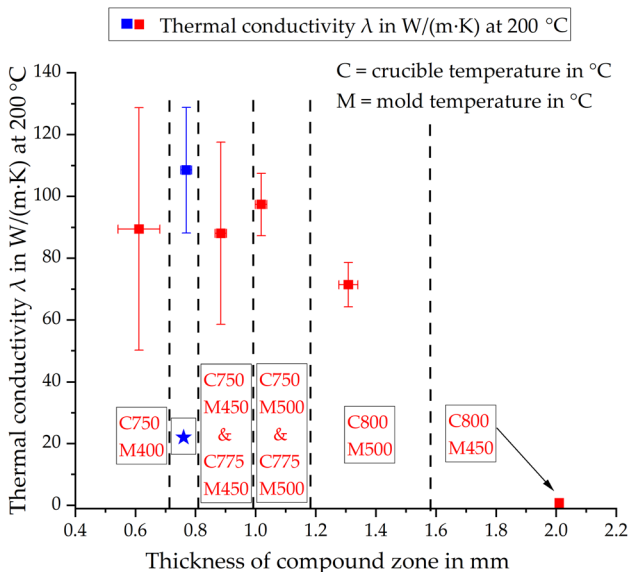
Figure 7. Diffraction patterns of the XRD analyses at the measurement points (MP) marked in Fig. 2.

Figure 10. Combined thermal conductivity of pure aluminum and the compound zones, mean values with n = 3.

thermal conductivity of cast aluminum (234.7 W/(m·K)). Hence, in order to create the highest possible thermal conductivity, the total thickness of the compound zone should approach zero. Although the thermal conductivities demonstrated in Figure 10 are high, they still turn out to be substantially lower than the thermal conductivity of the cast pure aluminum. The highest thermal conductivities of about 125 W/(m·K) were obtained for the "C775/M350" and "C750/M400" specimens.

The relationship between thermal conductivity and thickness of the compound zone at 200 °C, which is the maximum applicable temperature for aluminum-copper compounds before phases start growing permanently by diffusion, is summarized in Figure 11. Lower casting temperatures (left side of Figure 11) lead to a smaller thickness of the compound zone and hence to a lower contact resistance, which in turn results in a higher combined thermal conductivity. The error bars mark the scatter of the individual measurements. It is evident that different casting parameters can result in almost identical thicknesses of the compound zones but different thermal conductivities. For example, eight different samples with mold temperatures between 350 and 400 °C and crucible temperatures between 750 and 800 °C all showed similar compound zone thicknesses between 0.73 mm and 0.78 mm (standard deviation of $\pm$ 20 μm). Yet, the thermal conductivities of those samples varied from 74 to 132 W/(m·K). Moreover, the standard deviation of the thermal conductivity was larger at lower casting temperatures. This indicates that here the metallurgical bond could no longer be fully established.

Discussion

The obtained data on thermal conductivity show that one of the previous limitations of compound casting of aluminum and copper could be resolved. By doping monosilane into the inert gas atmosphere, the strong oxidation tendency of copper at elevated temperatures[15] often resulting in copper oxide inclusions at the interface between copper and aluminum[29] was successfully prevented. In order to form a compound casting featuring a strong metallurgical bond,[30] the aluminum casting alloy has to be liquid at the contact zone for a certain time. The introduced heat causes diffusion and finally results in a hypereutectic aluminum-copper melt directly in front of the copper melt interface.[22] Yet local temperature fluctuations affect the transport processes, leading to varying thicknesses of the compound zone. The diffusion of aluminum atoms into the surface of the copper piece lowers the melting point, and the copper at the interface finally starts melting as a result of the heat input from the liquid aluminum. Given the presence of the precipitates on the copper side, the diffusion of the copper atoms resulted in a hypereutectic melt. The eutectic microstructure was formed after the temperature dropped below the eutectic temperature. Based on the phase diagram, the first layer should form after the second. According to Tavassoli et al.,[22] the second layer precipitates mainly consist of the θ-phase (Al$_2$Cu). This incoherent phase forms globular precipitates as shown by Roos et al.[31] Accordingly, there was an enhanced intensity of the θ-phase pattern at MP 3 (Figure 7). This indicates that the diffusion of copper atoms into the still liquid cast aluminum resulted in a hypereutectic melt, leading to nucleation of the θ-phase at the copper interface upon cooling. The change in thickness as well as microstructure of the second layer at different casting parameters indicates that its formation can be prevented by selective adjustment of the casting parameters, resulting in a eutectic alloy in the

Figure 11. Thermal conductivity in relation to the compound zone thickness; ★: marks different casting parameters resulting in similar compound zone thickness, see main text for details.

compound zone. Consequently, the preheating temperature of the copper insert seems to have a more significant influence on the total thickness of the layers in the compound zone than the melt temperature. This can be attributed to the high thermal conductivity of copper.

It was observed that different casting parameters lead to different results regarding the formation of the third layer. With higher concentrations of copper in the resulting phases, the thermal conductivity decreases.[32] Specifically, high copper insertion temperatures as compared to the temperature of the melt lead to an increased thickness of the third layer. This can be attributed to the formation mechanism of the third layer, since it is formed as a result of the diffusion of copper atoms into the already solidified θ-phase.[22,33] Besides the already mentioned phases, Tavassoli et al.[22] identified the phases ζ (Al$_3$Cu$_4$) and δ (Al$_2$Cu$_3$) for melt temperatures of 800 °C. The phases were identified based on the chemical composition, but no verification of these phases with XRD was performed. In Figure 6 (c) an unidentified phase (*) in the compound zone can be spotted, which could be either the phase ζ (Al$_3$Cu$_4$) or δ (Al$_2$Cu$_3$). Pintore et al. also reported the presence of a rather broad Al$_3$Cu$_4$ phase in their Al-Cu compound castings.[29] Fu et al.[34] argued for the sole occurrence of the phases η$_2$ and δ. Jiang et al.[17] determined and verified the γ-phase using XRD. The occurrence of the η$_2$-phase between the γ- and θ-phase is controversial in current research. Zare et al.[13] and Tavassoli et al.[22] have determined its occurrence based on the chemical composition. Using the same approach, Liu et al.[15] were able to show a similar chemical composition of the mentioned phases. However, the more detailed examination of the third layer by electron back-scatter diffraction (EBSD) has revealed that the η$_2$-phase is probably a two-phase mixed structure of the γ- and θ-phase. By contrast, the EBSD images of the third layer in Jiang et al.[17] appear to indicate the presence of the η$_2$-phase. The formation of the different phases at the interface between the joining parts lowers the free Gibbs enthalpy of the system, which provides a driving force even in absence of a temperature gradient. In fact, the good thermal conductivity of the copper insert ensures that temperature gradients are low in the zone within which the intermetallic phases form. Earlier literature has already demonstrated that the phases do grow under isothermal conditions at temperatures as low as 495 °C,[35] i.e. in the completely solidified state.

The effect of the overall composition ratio of Al to Cu on the thermal conductivity has also been investigated earlier. The data reported by Ho et al.[32] indicates that minimal thermal conductivity (< 50 W/m·K) is reached for copper alloys containing between 70%–95% aluminum. Nevertheless, the influence of the multiphase intermetallic compound on the overall thermal conductivity is difficult to separate from others, since there is currently no way to measure the thermal properties of the individual phases

formed in the manufactured compound castings. This issue should be addressed in future work, as findings in this matter could contribute significantly to the further improvement of the casting process.

Klose et al. compared the thermal conductivities of conventional heat sinks with and without thermal paste with data obtained for aluminum-copper compounds produced by a high pressure die casting process. In that study, Zn-based coatings were applied to the copper surface prior to casting to allow for metallurgical bonding in spite of the process being conducted in normal (oxidizing) atmosphere.[2] In Figure 12, the results of the current study are compared with the results of Klose et al. as well as those of industrial methods such as soldered connections between the copper and aluminum.[25] To emphasize the effect of the casting parameters employed, both the data from the experiments that led to the low thermal conductivity (49–78 W/(m·K)) and the ones that resulted in smaller compound zone thickness and high thermal conductivity (≈ 125 W/(m·K) are included. It is immediately evident that the metal-to-metal contact achieved in the XHV-adequate atmosphere allowed for much higher thermal conductivity compared with conventional mechanical connections with or without thermal paste. Even the aluminum-copper compounds with a compound zone thickness of 2010 μm produced in the XHV-adequate environment had significantly higher thermal conductivities than the conventional heat sinks with and without thermal paste between the joining partners. When using moderate to low temperatures for both the mold (350 °C–400 °C) and the crucible (750 °C–775 °C), much thinner compound zones (732 μm / 773 μm) and very high combined thermal conductivity could be realized (≈ 125 W/(m·K)).
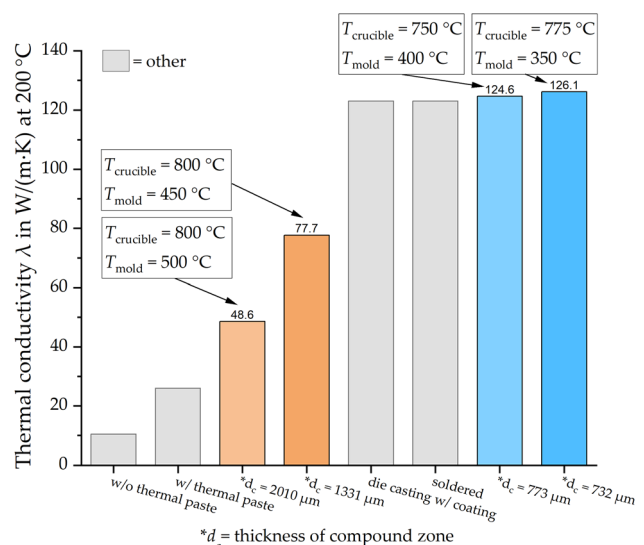
Figure 12. Comparison of the data obtained in the present study (orange and blue) in comparison to literature results from Refs.2,25 (in gray).

The phase diagram shows the compositions of the different phases in the third layer hardly changing with temperature, which can also be observed in the EDS line scans. Accordingly, the thermal conductivity of the third layer is clearly dominated by the thickness of this zone. The thicknesses and the microstructures of the other layers change with temperature, and it is not yet clear which effect is responsible for this phenomenon. However, data on electrical conductivity, which can be correlated with thermal conductivity, suggest that the overall thermal conductivity is governed by the behavior of the intermetallic compound and the eutectic zone. In this context, Pintore et al. observed a distinct correlation between increasing electrical resistance and increasing thickness of the eutectic area of their Al-Cu compound castings.[36] This effect also depended on substrate temperatures, which had a roughly similar influence on phase formation as the mold temperature regimes in the current study. Although the gravity die casting process employed here already allowed for thermal conductivities at least on a par with those of coated samples or soldered ones (Figure 12), it can be expected that these values could be improved if a further reduction of the still relatively thick intermetallic phase seam and the eutectic could be achieved. A viable approach appears to be tailoring the heat dissipation through the mold such as to inhibit the growth of the different layers during the compound casting process.

Conclusions

In order to achieve high thermal conductivity, which is of great interest for many highly effective cooling components made of aluminum and copper, a novel compound casting process was developed. Pure aluminum was cast onto a solid pure copper insert in an atmosphere adequate to extreme high vacuum (oxygen-free) to prevent re-oxidation of a de-oxidized copper insert as well as oxidation of the aluminum melt. The results of the present study can be summarized as follows:

1. Light and electron microscopic investigations of the compounds showed that an oxide-free, metallurgical bond was successfully established between the two materials. In the XHV-adequate atmosphere, aluminum bonds to copper without using coatings or fluxes. Thus, with counteracting the strong tendency of copper to oxidize at elevated temperatures, a major limitation of compound casting, could be overcome by doping monosilane into the inert gas atmosphere.
2. The thermal conductivity measurements showed that similar or even better results compared to those of conventional processes of joining aluminum and copper were achieved.

3. With decreasing casting temperatures ($T_{crucible}$ and T_{mold}), the compound zone thickness decreased, and consequently the thermal conductivity increased. Casting parameters of $T_{crucible} = 750$ °C and $T_{mold} = 400$ °C as well as $T_{crucible} = 775$ °C and $T_{mold} = 350$ °C resulted in the highest thermal conductivity of about 125 W/(m·K).
4. The layers detected using electron microscopy and X-ray diffraction starting from aluminum were: an eutectic structure of copper-rich aluminum solid solutions along with the θ-phase (Al_2Cu), precipitates from the θ-phase, and finally the η_2 (AlCu) and γ (Al_4Cu_9) intermetallic phases.

Data availability

Data are available from the authors upon request.

REFERENCES

1. G. Elger, R. Lauterbach, K. Dankwart, C. Zilkens, Inline thermal transient testing of high power LED modules for solder joint quality control, in proceedings of the 61st electronic components and technology conference, pp. 1649–1656 (2011)
2. C. Klose, P. Freytag, M. Otten, S.E. Thürer, H.J. Maier, Adv. Eng. Mater. **20**, 1701027 (2018). https://doi.org/10.1002/adem.201701027
3. S.D. Chen, A.K. Soh, F.J. Ke, Scripta Mater. **52**, 1135–1140 (2005). https://doi.org/10.1016/j.scriptamat.2005.02.004
4. K.S. Lee, Y.N. Kwon, Solid-state bonding between Al and Cu by vacuum hot pressing. Trans. Nonferrous Met. Soc. China **23**, 341–346 (2013). https://doi.org/10.1016/S1003-6326(13)62467-X
5. I. Hordych, K. Barienti, S. Herbst, H.J. Maier, F. Nürnberger, Metals **11**, 917 (2021). https://doi.org/10.3390/met11060917
6. M. Abbasi, A. Karimi Taheri, M.T. Salehi, J. Alloy. Compd. **319**(1), 233–241 (2001). https://doi.org/10.1016/S0925-8388(01)00872-6
7. L.Y. Sheng, F. Yang, T.F. Xi, C. Lai, H.Q. Ye, Compos. Part B-Eng. **42**, 1468–1473 (2011). https://doi.org/10.1016/j.compositesb.2011.04.045
8. C.Y. Chen, W.S. Hwang, Mater. Trans. **48**, 1938–1947 (2007). https://doi.org/10.2320/matertrans.MER2006371
9. S. Berski, Z. Stradomski, H. Dyja, J. Achiev. Mater. Manuf. Eng. **22**, 73–76 (2007)
10. A.G. Mamalis, A. Szala, N.M. Vaxevanidis, D.E. Manolakos, J. Mater. Process. Tech. **83**, 48–53 (1998). https://doi.org/10.1016/S0924-0136(98)00042-9
11. S. Khoddam, L. Tian, T. Sapanathan, P.D. Hodgson, A. Zarei-Hanzaki, Adv. Eng. Mater. **20**, 1800048 (2018). https://doi.org/10.1002/adem.201800048
12. A. Khosravifard, R. Ebrahimi, Mater. Design **31**, 493–499 (2010). https://doi.org/10.1016/j.matdes.2009.06.026
13. G.R. Zare, M. Divandari, H. Arabi, Mater. Sci. Tech. **29**, 190–196 (2013). https://doi.org/10.1179/1743284712Y.0000000096
14. K. Papis, B. Hallstedt, J.F. Löffler, P.J. Uggowitzer, Acta Mater. **56**, 3036–3043 (2008). https://doi.org/10.1016/j.actamat.2008.02.042
15. T. Liu, Q. Wang, Y. Sui, Q. Wang, W. Ding, Mater. Design **89**, 1137–1146 (2016). https://doi.org/10.1016/j.matdes.2015.10.072
16. A.O. Bakke, L. Arnberg, Y. Li, Mater. Sci. Eng. A **810**, 140979 (2021). https://doi.org/10.1016/j.msea.2021.140979
17. W. Jiang, F. Guan, G. Li, H. Jiang, J. Zhu, Z. Fan, Mater. Manuf. Process. **34**, 1016–1025 (2019). https://doi.org/10.1080/10426914.2019.1615084
18. A. Lange, Verbundgießen für Anwendungen in der Verschleißtechnik, PhD Dissertation, Magdeburg University (1999)
19. A.O. Bakke, J.O. Løland, S. Jørgensen et al., Interfacial microstructure formation in Al7SiMg/Cu compound castings. Inter. Metalcast **15**, 40–48 (2021). https://doi.org/10.1007/s40962-020-00463-w
20. U. Holländer, D. Wulff, A. Langohr, K. Möhwald, H.J. Maier, Int. J. Pr. Eng. Man.-G.T. **7**, 1059–1071 (2020). https://doi.org/10.1007/s40684-019-00109-1
21. H.J. Maier, S. Herbst, B. Denkena, M.A. Dittrich, F. Schaper, S. Worpenberg, R. Gustus, W. Maus-Friedrichs, Metals **10**, 1161 (2020). https://doi.org/10.3390/met10091161
22. S. Tavassoli, M. Abbasi, R. Tahavvori, Mater. Design **108**, 343–353 (2016). https://doi.org/10.1016/j.matdes.2016.06.076
23. R.D. Cowan, J. Appl. Phys. **34**, 926–927 (1963). https://doi.org/10.1063/1.1729564
24. H.D. Baehr, K. Stephan, in *Wärme- und stoffübertragung*. ed. by H.D. Baehr, K. Stephan (Springer, Berlin, 2016), pp.121–310
25. P. Freytag, Entwicklung stoffschlüssiger Aluminium-Kupfer-Verbunde im Verbundguss, PhD Dissertation, Leibniz University Hannover (2019)
26. T. Greß, V. Glück Nardi, T. Mittler et al., Interface formation and characterization of brass/aluminum compounds fabricated through die casting and semi-continuous casting. Inter. Metalcast **14**, 564–579 (2020). https://doi.org/10.1007/s40962-019-00387-0
27. S. Gates-Rector, T. Blanton, Powder Diffr. **34**, 1–9 (2019). https://doi.org/10.1017/S0885715619000812
28. M. Draissia, M.Y. Debili, Cent. Eur. J. Phys. **3**, 395–408 (2005). https://doi.org/10.2478/BF02475646
29. M. Pintore, O. Starykov, T. Mittler et al., Experimental investigations on the influence of the thermal conditions during composite casting on the microstructure of cu–al bilayer compounds. Inter. Metalcast **12**, 79–88 (2018). https://doi.org/10.1007/s40962-017-0140-0
30. B. Buchmayr, T. Weligoschek, Berg- hüttenmänn. Monatsh. **155**, 318–324 (2010). https://doi.org/10.1007/s00501-010-0582-7
31. E. Roos, K. Maile, M. Seidenfuß, *Werkstoffkunde für Ingenieure*, 6th edn. (Springer, Berlin, 2017), pp.250–259
32. C.Y. Ho, M.W. Ackerman, K.Y. Wu, S.G. Oh, T.N. Havill, J. Phys. Chem. Ref. Data **7**, 959–1177 (1978). https://doi.org/10.1063/1.555583
33. Y. Han, L. Ben, J. Yao, S. Feng, C. Wu, Int. J. Miner. Metall. **22**, 309–318 (2015). https://doi.org/10.1007/s12613-015-1075-1

34. Y. Fu, Y. Zhang, J. Jie, K. Svynarenko, C. Liang, T. Li, China Foundry **14**, 194–198 (2017). https://doi.org/10.1007/s41230-017-6057-7

35. Y. Funamizu, K. Watanabe, Interdiffusion in the Al–Cu system. Trans. Jpn. Inst. Met. **12**, 147–152 (1971). https://doi.org/10.2320/MATERTRANS1960.12.147

36. M. Pintore, J. Wölck, T. Mittler et al., Composite casting and characterization of Cu–Al bilayer compounds. Inter. Metalcast **14**, 155–166 (2020). https://doi.org/10.1007/s40962-019-00344-x